



Discovery and Optimization of Nonpeptide HIV-1 Protease Inhibitors

Peter J. Tummino,^{a,*} J. V. N. Vara Prasad,^b Donna Ferguson,^a Carolyn Nouhan,^a Neil Graham,^a John M. Domagala,^b Edmund Ellsworth,^b Christopher Gajda,^b Susan E. Hagen,^b Elizabeth A. Lunney,^b Kimberly S. Para,^b Bradley D. Tait,^b Alexander Pavlovsky,^b John W. Erickson,^d Stephen Gracheck,^c Thomas J. McQuade^c and Donald J. Hupe^a

Departments of ^aBiochemistry, ^bChemistry, and ^cInfectious Diseases, Parke-Davis Pharmaceutical Research, Division of Warner-Lambert Company, Ann Arbor, MI 48105, U.S.A.

^dStructural Biochemistry Program, NCI-Frederick Cancer Research and Development Center, PRI/DynCorp, Frederick, MD 21702, U.S.A.

Abstract—Several small, achiral nonpeptide inhibitors of HIV-1 protease with low micromolar activity were identified by mass screening of the Parke-Davis compound library. Two of the compounds, structurally similar, were both found to be competitive and reversible inhibitors [compound **1**, 4-hydroxy-3-(3-phenoxypropyl)-1-benzopyran-2-one: $K_i = 1.0 \mu\text{M}$; compound **2**, 4-hydroxy-6-phenyl-3-(phenylthio)-pyran-2-one: $K_i = 1.1 \mu\text{M}$]. These inhibitors were chosen as initial leads for optimization of in vitro inhibitory activity based on molecular modeling and X-ray crystallographic structural data. While improvements in inhibitory potency were small with analogues of compound **1**, important X-ray crystallographic structural information of the enzyme-inhibitor complex was gained. When bound, **1** was found to displace H₂O301 in the active site while hydrogen bonding to the catalytic Asps and Ile50 and Ile150. The pyranone group of compound **2** was found to bind at the active site in the same manner, with the 6-phenyl and the 3-phenylthio occupying P1 and P1', respectively. The structural information was used to develop design strategies to reach three or four of the internal pockets, P2–P2'. This work led to analogues of diverse structure with high potency ($\text{IC}_{50} < 10 \text{ nM}$) that contain either one or no chiral centers and remain nonpeptidic. The highly potent compounds possess less anti-HIV activity in cellular assays than expected, and current optimization now focuses on increasing cellular activity. The value of the HIV-1 protease inhibitors described is their potential as better pharmacological agents with a different pattern of viral resistance development, relative to the peptidic inhibitors in human clinical trials. Copyright © 1996 Elsevier Science Ltd

Introduction

The human immunodeficiency virus (HIV) is the causative agent of acquired immunodeficiency syndrome, AIDS. The virally-encoded aspartic protease of HIV has been extensively studied as a promising chemotherapeutic target for AIDS for several reasons. The HIV protease, which is responsible for the proteolysis of gag and gag/pol polyproteins to mature structural proteins and enzymes, is necessary for the production of infectious virions in cell culture. HIV containing a mutation that encodes for an inactive protease has been found to yield noninfectious virions,¹ and inhibitors specific for the viral protease have been shown to inhibit viral replication.² HIV protease is a member of the aspartic protease family and knowledge about structure, enzymology, and inhibitor design for these proteases greatly facilitated initial development of HIV protease inhibitors.³ Specifically, the knowledge accumulated in the design of inhibitors against the aspartic protease renin accelerated HIV protease inhibitor design⁴. Finally, co-crystallization of the retroviral protease, which is a 22 kD homodimer, with inhibitors and subsequent structure determination has

not encountered unusual difficulties. For this reason, a large effort in X-ray crystallographic studies of HIV protease/inhibitor complexes has made the protease the most structurally characterized protein with hundreds of structures determined (many remain proprietary in pharmaceutical drug discovery efforts).^{5,6}

Peptidic and peptidomimetic nonhydrolysable transition state mimics were rapidly developed as highly potent HIV protease inhibitors (for reviews, see ref 7 and 8). These competitive inhibitors possess optimal interactions in substrate binding pockets from P3 to P3' (nomenclature from Schechter and Berger⁹), with low to subnanomolar K_i values. However, their peptidic nature often makes them poor pharmacological agents, with low bioavailability and rapid clearance.^{8,10} Several of the peptidic inhibitors are currently in clinical trials (examples include Ro 31-8959,¹¹ MK-639,¹² and ABT-538¹³) while significant efforts to improve their pharmacology continue.

The goal of our efforts was to identify small nonpeptide HIV protease inhibitors with potentially better pharmacological characteristics, and employ structural information about the enzyme-inhibitor complex to design analogues that possess the necessary in vitro potency. Lam and co-workers have employed this

Key words: HIV protease, nonpeptide inhibitor, pyran-2-ones, 5,6-dihydropyran-2-ones, structure-based design.

strategy to design a nonpeptide series based on the structural features of peptidic inhibitors bound to the enzyme.¹⁴ The inhibitors are highly potent against the enzyme and against HIV in cell culture. Our group identified nonpeptide inhibitors by screening the Parke–Davis compound library. This yielded several small, structurally distinct, achiral nonpeptides with low micromolar inhibitory activity, two of which served as starting points for structure-based design. These inhibitors were found to bind in a unique manner relative to their peptidic counterparts. Starting with one of the compounds, the iterative process of inhibitor design and synthesis, biochemical evaluation, and structure determination was used successfully to generate compounds with low nanomolar potency in two related series. Described herein is the discovery and characterization of the initial nonpeptide leads, along with their structure-based optimization into potent HIV-1 protease inhibitors.

Results and Discussion

Results from mass screening and biochemical characterization

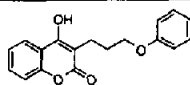
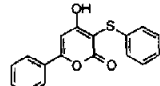
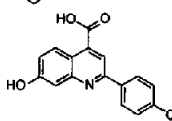
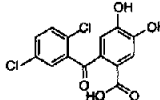
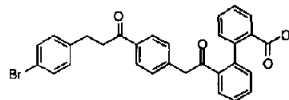
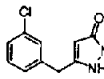
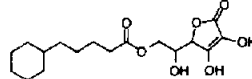
The screening of the Parke–Davis compound library was accomplished using a general strategy for lead discovery that has been applied to many enzyme targets. An initial high through-put assay was established which allowed large numbers of samples to be examined, even at the expense of accuracy of the inhibition data. A scintillation proximity assay was used which gave a decreasing signal in the presence of HIV-1 protease, due to cleavage of radioactively labeled substrate attached covalently to a scintillant-containing bead. This method allowed for the rapid screening of approximately 150,000 compounds delivered in mixtures of 10 compounds per sample in DMSO solution. These samples arrived in 96-well format in 2 μ L amounts, so that only addition of assay mix, enzyme and beads by robot was required to generate the data, without any separation step. Approximately 200 compounds were confirmed as actives from the screen.

The active compounds were further characterized in a more quantitative manner by determining IC_{50} values using an HPLC assay, as previously described.¹⁵ Part of the lead selection process, which reflects the value of repetitively screening the same collection with various enzymes, was the recognition of classes of compounds that repeatedly appear as inhibitors, and are therefore of less interest. In the case of HIV protease, some classes of 'inhibitors' were eliminated because their apparent activity was due to enzyme precipitation caused by the insoluble compounds. Therefore, a simple estimation of micromolar solubility¹⁵ allowed for elimination of these compounds. This work led to the identification of seven series of nonpeptide HIV-1 protease inhibitors, representative compounds of which are shown in Table 1. The compounds are small, achiral (with the exception of compound 7), nonpep-

tidic, and demonstrate low μ M protease inhibition reproducibly. The fact that these compounds were identified from one compound library is noteworthy, since they are structurally distinct from their peptidic counterparts, and since they represent a large proportion of all the reported nonpeptide HIV-1 protease inhibitors (review by S. Thaisrivongs¹⁶). A structural analogue of **4** was previously reported as an HIV protease inhibitor, with a similar IC_{50} value.¹⁷ Each of the seven compounds is a reasonable starting point for a structure-based design effort. While the majority of HIV protease inhibitor efforts have focused on peptidic compounds, the inhibitors in Table 1 demonstrate the utility of mass screening to identify nonpeptide inhibitors as initial leads.

Further inhibitory characterization of the series represented by the compounds **1**, **2**, and **5** was carried out. Compounds **1**, **2**, and **5** were found to inhibit in a competitive manner. A double reciprocal plot for inhibition by **2** is shown in Figure 1, which clearly demonstrates competitive inhibition with a $K_i = 1.1 \mu$ M. Similar kinetic analyses of **1** ($K_i = 1.0 \mu$ M¹⁵), analogues of **5**¹⁸ and more potent analogues of **2**¹⁹ have all exhibited competitive inhibition. Thus, these three classes of inhibitors compete with substrate for binding to the enzyme active site as has been found for peptidic inhibitors. Compounds **1** and **2** were also found to be fast-binding and reversible, while **5** inhibits in a reversible slow-binding manner. The time-dependent inhibition of HIV-1 protease by compound **5** is shown in Figure 2 fit to the integrated first-order rate equation, with $k_{on} = 0.18 \mu$ M⁻¹min⁻¹, $k_{off} = 9.7 \times 10^{-2} \text{ min}^{-1}$ and $K_i = 0.14 \mu$ M. A limited structure–activity relationship (SAR) derived from

Table 1. Structures and IC_{50} values of mass screen hits

Structure	Compd	IC_{50} (μ M)
	1	2.3
	2	3.0
	3	6.9
	4	8.1
	5	19
	6	29
	7	29

mass screen hits identified one substituent on compound **5** that was essential for inhibitory activity: the biphenyl carboxylic acid.¹⁸ Although **5** is more potent, compounds **1** [4-hydroxy-3-(3-phenoxypropyl)-1-benzopyran-2-one] and **2** [4-hydroxy-6-phenyl-3-(phenylthio)pyran-2-one] were chosen for structure-based optimization of inhibitory activity for several reasons. Analogues of these small, achiral compounds were accessible synthetically, and a small coherent SAR was generated around **1** and **2** from Parke-Davis sample collection compounds. Both inhibitors possess a 4-hydroxypyranone core essential for inhibitory activity, and a model for its mode of binding to the enzyme active site was proposed (to be discussed subsequently). The initial strategy for inhibitory activity optimization in both series was to explore the SAR while molecular modeling and X-ray crystallographic studies were being conducted on the parent compounds.

4-Hydroxybenzopyranones

Molecular modeling and X-ray crystallographic studies of compound **1** bound to HIV-1 protease were performed, and the results have been described in detail previously.²⁰ In modeling the binding of **1**, there was uncertainty as to whether the inhibitor would displace the two active site water molecules. 'H₂Ocat' is hydrogen-bonded to the catalytic Asp carboxylates and is proposed to be involved in the catalytic amide bond hydrolysis.²¹ H₂O301 is present in peptidomimetic inhibitor/enzyme complexes in a hydrogen-bonding network between the ligand and the amide nitrogens of Ile50 and Ile150 in the flap of the enzyme.⁵ Since there was no precedent for the mode of binding for this nonpeptide ligand, the modeling was performed with two, one or no water molecules present in the complex. The X-ray crystallographic structure solved to 3.0 Å

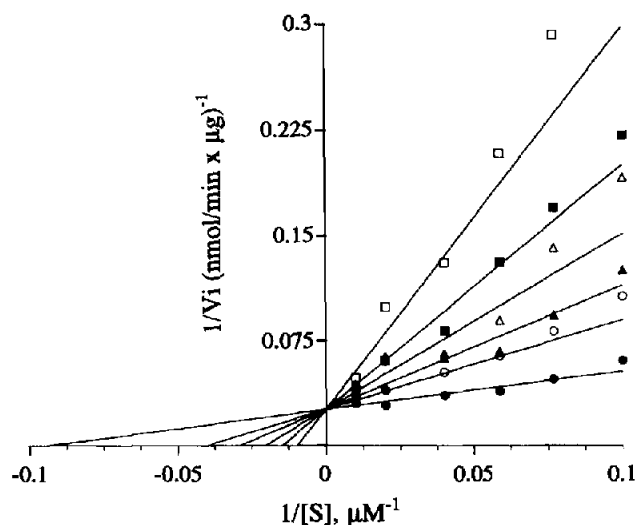


Figure 1. Double reciprocal plot for inhibition of HIV-1 protease by compound **2**. Inhibitor concn, μM : (\square) 10, (\bullet) 6.0, (\triangle) 4.0, (\blacktriangle) 2.5, (\circ) 1.5, (\bullet) 0.0. The data is shown fit to the equation for competitive inhibition ($V_i = k_{\text{cat}}[S]/([S] + K_m(1 + [I]/K_i))$) by a nonlinear least-squares algorithm, with $K_m = 10.6 \pm 1.7$ (std error) μM , $k_{\text{cat}} = 14.1 \pm 0.62 \text{ s}^{-1}$ and $K_i = 1.1 \pm 0.18 \mu\text{M}$.

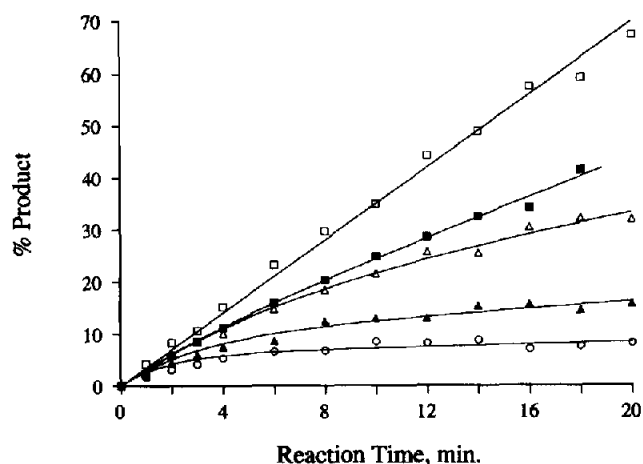
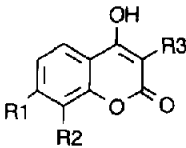


Figure 2. Time-dependent inhibition of HIV-1 protease by compound **5**. The % conversion to product versus reaction time was measured as a function of inhibitor concn, μM : (\square) 0.0, (\blacksquare) 2.0, (\triangle) 4.0, (\blacktriangle) 8.0, (\circ) 16. [Protease] = 4.2 nM, [substrate] = 80 μM . The data was fit to the integrated first-order rate equation,⁴¹ $y = v_s \cdot x + (v_o - v_s)(1 - \exp(-k_{\text{obs}} \cdot x))/k_{\text{obs}}$, by a nonlinear least-squares algorithm to yield values of k_{obs} , v_o , and v_s at each inhibitor concentration. k_{obs} values were plotted versus $[I]$ (not shown), and fit to the equation $k_{\text{obs}} = k_{\text{off}} + k_{\text{on}} [I]/(1 + [S]/K_m)$, $k_{\text{on}} = 0.18 \mu\text{M}^{-1}\text{min}^{-1}$ and $k_{\text{off}} = 9.7 \times 10^{-2} \text{ min}^{-1}$. Values for v_o and v_s were plotted as $(v_o - v_s)/v_s$ versus $[I]$ (not shown), and fit to the equation $v_o - v_s/v_s = [I]/K_i(1 + [S]/K_m)$, $K_i = 0.14 \mu\text{M}$.

demonstrated that both water molecules are displaced by **1**, and the structure was in good agreement with the unsolvated structure from molecular modeling. The 4-hydroxyl of the ligand displaces H₂Ocat and is within hydrogen-bonding distance of both catalytic Asp carboxylates (Asp25 and Asp125). The lactone of the benzopyranone of **1** displaces H₂O301 and is within hydrogen bonding distance of the amide nitrogens of Ile50 and Ile150. The fused phenyl ring of the benzopyranone is oriented in the P1 pocket. The phenoxypropyl group was found in two conformations, either occupying the P2' or P3' pocket. The finding that compound **1** displaces H₂O301, which is not true for any of the peptidic inhibitors, indicated that the inhibitor binds at the enzyme active site in a unique manner. It has been suggested that displacement of H₂O301 may confer inhibitory and specificity advantages.^{22,23}

Several interesting analogues of **1** were identified in the mass screen, and shown in Table 2. Compound **8** demonstrates the importance of the phenoxypropyl group of **1** to inhibitory activity. That activity is restored with the analogues **9** and **10**. Compound **9** is warfarin, which has been used as a therapeutic agent in humans in the treatment of thrombo-embolic disease with greater than 95% absorption after oral administration.²⁴ Compound **10**, a warfarin analogue, was found to be ninefold more potent than the parent compound. Our group²⁵ and P. Tomich and K. Watenpaugh at Upjohn²⁶ independently identified these same compounds as HIV-1 protease inhibitors. Warfarin analogues appear to possess a structural advantage over **1**. As stated above, compound **1** was found to bind in two conformations, with the 3-phenoxypropyl group

Table 2. Inhibitory activity of 4-hydroxy-coumarins


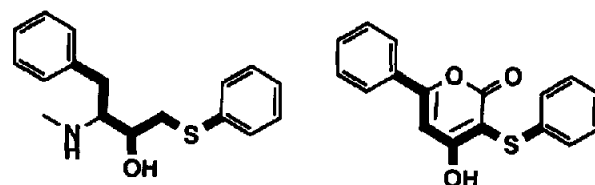
Compd	R ₁	R ₂	R ₃	IC ₅₀ (μM)
1	H	H	(CH ₂) ₃ OPh	2.3
8	H	H	CH ₂ Ph	120
9	H	H	CH(Ph)CH ₂ COCH ₃	18
10	CH ₃	CH ₃	CH(Ph)CH ₂ COCH ₃	1.9
11	H	H	(CH ₂) ₃ SPh	26
12	H	H	(CH ₂) ₄ Ph	110
13	H	H	(CH ₂) ₄ -Ph(2-OCH ₃)	1.7
14	H	H	(CH ₂) ₄ -Ph(4-OCH ₃)	> 100
15	OH	H	(CH ₂) ₄ -Ph(2-OCH ₃)	0.52

either extending to the P3' pocket or occupying the P2' site. Since the warfarin analogues have a branched group at the 3-position, it is possible for these molecules to reach both pockets simultaneously. While our group did not pursue warfarin analogues, the Upjohn group found that these analogues do bind in two P' pockets,²⁷ and were able to successfully optimize activity to yield an analogue with $K_i = 15$ nM.²⁸

Replacement of the oxygen in the phenoxypropyl group of **1** with sulfur (**11**) or carbon (**12**) decreases activity, indicating the importance of the oxygen to inhibitory activity. Incorporation of an oxygen in **12** at a position proximal to the phenoxy oxygen of **1** with an *o*-methoxy group restored inhibitory activity (**13**), while substitution of an oxygen at a more distant position through a *p*-methoxy group (**14**) did not. It was, therefore, expected that the phenoxypropyl oxygen of **1** would be involved in a polar interaction with the enzyme. However, this was not seen in the X-ray crystal structure. Modeling indicated that the oxygen ligand may be a part of a hydrogen-bonding network involving Gly48 or Asp29 and a water molecule. Compound **15** demonstrates improved activity due to the addition of a hydroxyl on the fused phenyl ring, which may make it a better mimic for Tyr, a residue found in the native sequence at the P1 site.²⁹

4-Hydroxy-6-phenylpyranones

Prior to the solution of the X-ray structure of **1** with HIV-1 protease, a binding mode for compound **2** was proposed by analogy with known transition-state analogues,³⁰ as shown in Figure 3. It was postulated that **2** may be analogous to a conformationally-restricted P1-P1' peptidomimetic, with its enolic hydroxyl moiety hydrogen-bonded to the two catalytic Asp residues and with the two phenyl groups occupying P1 and P1'. It was confirmed by X-ray crystallography that the 4-hydroxy-pyranone core of **16**, a close analogue of **2**, does bind to the enzyme as was postulated and in the same manner as the core of **1**³⁰ (Fig. 4). The 6-phenyl occupies the P1 pocket and the

**Figure 3.** Comparison of hydroxyethyl sulfide isostere with compound **16**.

benzylthio group reaches into P1'. The distances between specific groups of the inhibitor and enzyme residues are shown in Figure 5, as determined from the X-ray crystallographic data. Thus, compound **16** was a promising starting point for structure-based design since this small achiral compound bound at the HIV-1 protease core and displaced H₂O301. Compound **16** only binds in two of the active-site pockets (while peptidic compounds occupy as many as six pockets), and possesses moderate potency (IC₅₀ = 1.7 μM). Thus, the strategy was to maintain the 4-hydroxypyranone core while determining whether the P1 and P1' substituents were optimal, followed by extending the inhibitor to reach the P2, P2' and possibly P3, P3' pockets. This was to be accomplished without the addition of any peptidic character to the inhibitors.

Table 3 is a short summary of the progress made in the optimization of inhibitory activity of the 4-hydroxypyranones, resulting from structure-based design and synthesis of a large number of compounds. The detailed SAR has been described elsewhere.^{30,31} The addition of either one or two methylenes between the 3-S and the phenyl yields optimal activity as seen with **16** and **17**; longer aliphatic chains do not increase potency. The addition of a 4-hydroxy on the 6-phenyl as in **18** increases activity; an analogous observation was made with the benzopyranone **15**. Molecular modeling suggested that the P3 pocket might be reached from the 6-phenyl to obtain a favorable interaction with Arg108, and **19** was synthesized for that purpose. This analogue was found to have a significant improvement in inhibitory activity (IC₅₀ = 0.16 μM).

Optimization of the 3-phenylthio group lead to compounds **20–23**. Branched aliphatic substituents were added on the phenylthio group *ortho* to the sulfur, and molecular modeling indicated that these groups would occupy P1' with the 3-phenylthio group reaching into P2'. The addition of an *o*-methyl (**20**) or *o*-isopropyl (**21**), or *o*-*t*-butyl (**22**) was found to increase potency dramatically relative to the parent compound, **2**. For the *o*-*t*-butyl derivative, the addition of a 3-methyl on the phenyl in P1 (**23**) yielded another twofold increase in potency (IC₅₀ = 7.0 nM, K_i = 3.0 nM). The X-ray crystal structure of **21** was solved³¹ in order to determine how the isopropyl group affected inhibitor binding to the enzyme. As expected, the 4-hydroxypyranone core bound in the same manner as was found for compound **2** and the isopropyl group was found to occupy P1' with the phenylthio partially in the P2' pocket. These analogues possess greatly improved binding due to interactions in a third pocket



Figure 4. Relaxed stereo representation of the X-ray crystal structure of compound **16** (yellow) bound to HIV protease. Asp25/Asp125 (above) and Ile50/Ile150 (below) from the crystal structure are shown in cyan.

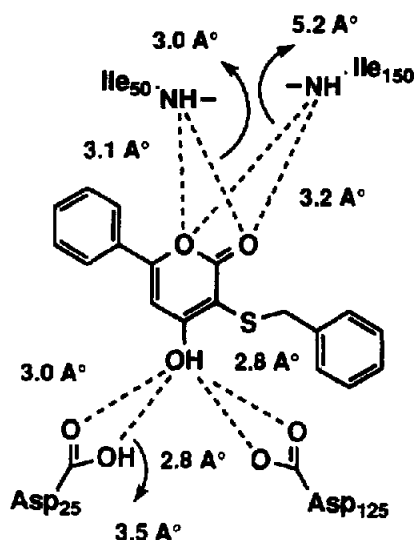
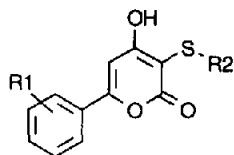


Figure 5. Interatomic distances of compound **16** bound to HIV protease in the X-ray crystal structure.

Table 3. Inhibitory activity of 4-hydroxy-6-phenylpyranones



Compd	R ₁	R ₂	IC ₅₀ (μM)
2	H	Ph	3.0
16	H	CH ₃ Ph	1.7
17	H	CH ₂ CH ₂ Ph	1.3
18	4-OH	CH ₂ CH ₂ Ph	0.52
19	4-OCH ₂ CO ₂ H	CH ₂ CH ₂ Ph	0.16
20	H	Ph(2-Me)	0.42
21	H	Ph(2- <i>i</i> Pr)	0.037
22	H	Ph(2- <i>t</i> Bu)	0.017
23	(3-Me)	Ph(2- <i>t</i> Bu)	0.007

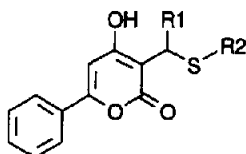
(P1–P2'). Compound **23** ($K_i = 3.0$ nM) is striking since it differs from the mass screen hit **2** by the simple addition of a *t*-butyl and a methyl group, yet is three orders of magnitude more potent. This low nanomolar compound is achiral, low molecular weight and can be synthesized in three steps.

4-Hydroxy-6-phenylpyranylthiomethanes

Another strategy pursued for the design of analogues that would occupy two P' pockets was to have a branched group at the C-3 position of the 4-hydroxy-pyranone core, similar to the warfarin derivatives. Analogues were synthesized with the sulfur in the β position and carbon in the α position, the site of branching with aromatic and aliphatic substituents, and results summarized in Table 4 (complete results previously described¹⁹). Compound **24**, with two phenyl substituents, shows improved activity over the pyranone **16**. Compounds **25** and **27** demonstrate about a twofold improvement with an isobutyl group on the C-branch instead of phenyl (**24** and **26**, respectively). This finding is consistent with the substituents at the P2' site of tight-binding substrates.³² These same inhibitors demonstrate that the benzyl group is preferred over phenyl on the S-branch. Cyclization of the isobutyl terminus to create a cyclopropylmethyl group in **28**, which provides π character, improved activity to IC₅₀ 84 = nM. Since there was literature precedent with the peptidic inhibitors for the use of modified amino acids containing cyclohexyl groups in P1',^{7,16} cyclic aliphatic groups were substituted on the S-branch (compounds **29–32**). Two of the four inhibitors have similar potency to the analogous compounds with the benzyl substituents (**27**, **28**). Although several of the branched pyranones possess good in vitro activity, they are generally less potent than the pyranones with a *t*-butyl substitution (**22**, **23**).

6,6-Disubstituted 5,6-dihydropyranones

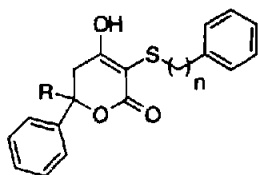
Since significant potency gains were made by increasing interactions in the P' pockets, a strategy was developed

Table 4. Inhibitory activity of 4-hydroxy-6-phenyl-pyranylthio-methanes

Compd	R ₁	R ₂	IC ₅₀ (μM)
24	Ph	Ph	0.78
25	Isobutyl	Ph	0.41
26	Ph	CH ₂ Ph	0.48
27	Isobutyl	CH ₂ Ph	0.26
28	CH ₂ -cyclopropyl	CH ₂ Ph	0.084
29	CH ₂ -cyclopropyl	Cyclohexyl	0.15
30	CH ₂ -cyclopropyl	Cyclopentyl	0.069
31	Isobutyl	Cyclopentyl	0.058
32	Cyclopentyl	Cyclopentyl	(K _i = 33 nM) 0.23

to optimize binding in P1 and P2. It had been shown that substituents on the 6-phenyl of **16** could be used to create interactions in the P3 pocket (compound **19**). However, analysis of the X-ray crystal structure of **16** indicated it was not feasible to substitute on the 6-phenyl and effectively reach P2. Molecular modeling showed that disubstitution at the 6-position following saturation of the 5,6 pyranone double bond would provide two groups that could reach P1 and P2 simultaneously. Synthesis and inhibitory activity of these 6,6-disubstituted 5,6-dihydropyranones has been previously described,^{33–37} and a brief summary of the SAR is shown in Tables 5 and 6. All of the compounds in Table 5 with a chiral center were tested as racemic mixtures.

Compound **33** has inhibitory activity comparable to the analogous pyranone (**17**). While a three-carbon alkyl straight chain decreases potency somewhat (**34**), the five-carbon straight (**35**) or branched (**36**) chain increases inhibitory activity greater than 20-fold. The addition of a terminal carboxylic acid functionality to

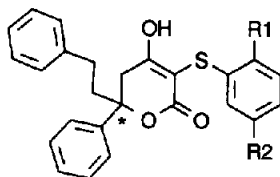
Table 5. Inhibitory activity of 6,6-disubstituted-5,6-dihydropyranones

Compd	n	R	IC ₅₀ (μM)
33	2	H	2.1
34	2	CH ₃ (CH ₂) ₂	5.1
35	2	CH ₃ (CH ₂) ₄	0.084
36	2	(CH ₃) ₂ CH(CH ₂) ₂	0.096
37	2	HO ₂ C(CH ₂) ₄	0.005
38	1	Ph	0.26
39	1	Ph(CH ₂) ₂	0.060

37 increased activity almost another 20-fold to IC₅₀ 5.0 nM. While modeling predicted the 6-phenyl would occupy P1, the acid group was incorporated in **37** for potential hydrogen bonding in P2 with the amides of Asp129/Asp130. In a close structural analogue of **37** [where the 3-S-phenethyl is replaced by a 3-S-(*o*-isopropyl)phenyl) group], the X-ray crystal structure indicated that the acid interacts through a shared proton with the side chain of Asp130. The potency gain observed may be due to this interaction. Analogues **38** and **39** have two aromatic substitutions at the 6-position, with the phenethyl favored over the phenyl. A larger SAR showed that the two-carbon length of the phenethyl is optimal, as predicted from molecular modeling for the substituent reaching into P2. For further analogue design, the substituents at the 6-position were chosen to be phenyl and phenethyl. The carboxylic acid straight-chain, although more potent, was not studied further due to concerns about decreased cell penetration with the charged compound.

With the 6,6-phenyl, phenethyl substituents kept constant, substitutions were made on the phenylthio identical to those described for the pyranones in Table 3 (both design efforts were performed in parallel). In this case, the disubstituted dihydropyranone (**40**) is greater than 20-fold more potent than the analogous monosubstituted pyranone (**2**), Table 6. The progression from methyl (**41**) to isopropyl (**42**) to *t*-butyl (**46**) showed the same incremental improvement with increasing size as was found for the pyranones. However, the magnitude of the increase in potency is smaller, such that the potent dihydropyranones **42** and **46** are only three to fivefold more potent than the analogous pyranones (**21** and **22**). The IC₅₀ values for these low nM compounds were confirmed by K_i determinations (data not shown), eliminating the possibility that the limits of detection for the *in vitro* assay had been reached. The relative potencies of these dihydropyranones and pyranones will be discussed subsequently with relation to the pH dependence of inhibition by these compounds. It was known from the X-ray structure of pyranone **21** bound to HIV-1 protease that the branched aliphatic group occupied P1'. Modeling indicated that the P2' position could be reached with a substituent *para* to the branched aliphatic. The optimal substituent in the *para* position for the isopropyl series was found to be a methyl group (**43**), while H is optimal for the *t*-butyl series (**46**, **47**). Since modeling predicted the 6-phenyl to occupy P1 and the 6-phenethyl to reach P2, it was expected that an *S*-configuration would be favored over *R* at the 6-position. The *S* enantiomer of **43**, which is **45**, was found to be 21-fold more active than the *R* enantiomer, **44**. A similar preference for the *S* configuration at the 6-position has been seen with other dihydropyranones (data not shown).

The X-ray crystal structure for **45** complexed with HIV-1 protease was determined, and its bound structure is shown overlaid with the symmetrical inhibitor A-74704²³ bound to the enzyme, shown in Figure 6. This figure illustrates two entirely different design

Table 6. Inhibitory activity of 6,6-disubstituted-5,6-dihydropyranones

Compd	*Chirality	R ₁	R ₂	IC ₅₀ (μM)
40	6- <i>R,S</i>	H	H	0.13
41	6- <i>R,S</i>	Me	H	0.073
42	6- <i>R,S</i>	Isopropyl	H	0.014
43	6- <i>R,S</i>	Isopropyl	Me	0.0073
44	6- <i>R</i>	Isopropyl	Me	0.13
45	6- <i>S</i>	Isopropyl	Me	0.0062
46	6- <i>R,S</i>	<i>t</i> -Butyl	H	0.0036
47	6- <i>R,S</i>	<i>t</i> -Butyl	Me	0.0098

approaches for interaction at P2–P2' and the catalytic core of HIV-1 protease. As was seen for the pyranone, the 4-hydroxyl of **45** is within hydrogen-bonding distance of the catalytic Asps, and the lactone of the pyranone ring hydrogen bonds to the amides of Ile50 and Ile150. The inhibitor A-74704 hydrogen bonds with the Ile amides also, but through H₂O301 shown in red (Fig. 6). H₂O301 overlaps with the lactone of **45**. The 6-phenyl of **45**, occupying P1, overlaps with the phenyl substituent of A-74704 in P1. The phenethyl group of **45** reaches into P2, shifted somewhat further out than the P2 group of A-74704. The *o*-isopropyl on the 3-phenylthio of **45** occupies P1', with the methyl *para* to this group reaching into P2'. The groups overlap well with the P1' and P2' substituents of A-74704. Compound **45** effectively reaches the four inner substrate pockets of the enzyme with interactions at the catalytic core without possessing any peptide amide bonds and with only one chiral center.

pH Dependence of inhibitory activity/cellular anti-HIV activity

The pyranones and dihydropyranones described do not possess submicromolar anti-HIV activity in cellular assays, despite several inhibitors exhibiting low nanomolar activity against the purified enzyme. This is in contrast to what has been reported for some of the peptidic inhibitors, which have low nanomolar in vitro activity and submicromolar cellular IC₅₀ values.⁸ An important contributor to the lack of potent antiviral activity may be the protonation state of the 4-hydroxyl

substituent on the pyranones and dihydropyranones. As described above, X-ray structural data indicates that the 4-hydroxyl group is within hydrogen-bonding distance of both catalytic Asps, and thus the protonation state of the 4-hydroxyl would have an impact on the binding affinity of the compound. The p*K_a* for this group in solution was found to be in the range 4–5 for many of the compounds. The in vitro assay was performed close to the pH optimum for the enzyme, at pH 4.7. To determine the inhibitory activity closer to the physiological pH of 7.4, selected compounds were assayed at pH 6.2. It should be noted that the protease is essentially inactive in vitro at pH 7.4. The results at the higher pH along with p*K_a* values and cellular anti-HIV data are shown in Table 7 (methods and data previously described¹⁹). The pyranone **21** demonstrates a 19-fold loss of potency at the higher pH. As might be expected, this pH-sensitive inhibitor has no measurable antiviral activity in the absence of toxicity. A similar decrease in inhibitory activity in vitro was seen for several analogues of **21**. Compound **21** has a sulfur in the 3-position while the branched pyranones **27**, **29**, and **32** have a carbon. The p*K_a* values of the latter compounds are about 2 units higher. The higher p*K_a* values correspond to little or no pH-dependent loss of in vitro activity and to micromolar antiviral activity in cells. Therefore, despite having significantly less potency than **21** at pH 4.7, the branched pyranones (**27**, **29**, and **32**) with higher p*K_a* values are active against HIV, possibly because they retain much of their inhibitory activity at physiological pH.

The dihydropyranones **42** and **47** (with sulfurs in the 3-position) have p*K_a* values similar to those of **21**, yet both compounds are significantly less pH-sensitive in vitro. While **42** was found to be not active in cells, **47** was not tested in this assay. The fact that **42** and **47** are much less pH-sensitive than **21**, despite possessing similar p*K_a* values in solution, points out that the relationship between the 4-hydroxyl p*K_a* and pH-dependence of inhibition is not direct. In fact, the p*K_a* of the hydrogen-bonding network between the 4-hydroxyl of the inhibitor and the catalytic Asps when the inhibitor is bound to the enzyme determines the pH dependence of inhibition of the compound. A better understanding of the pH dependence can be gained by measuring *K_i* values across a large pH range for a structurally diverse series of compounds. Interestingly, it has been reported previously that an HIV protease inhibitor with no ionizable group in the pH range still demonstrates pH dependence of inhibition, due to the different affinities the inhibitor has for the enzyme in different protonation states.³⁸ While the loss

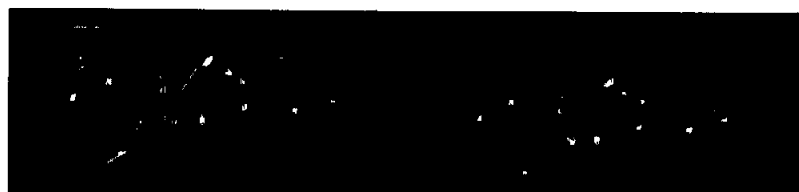


Figure 6. Relaxed stereo-representation of the X-ray crystal structure of compound **45** (yellow) bound to HIV protease overlaid with the crystal structure of the symmetrical inhibitor A-74704 (cyan) bound to the protease.²³

Table 7. pH Dependence of inhibitory activity, pK_a values and cellular anti-HIV activity of selected pyranones and dihydropyranones

Compd	IC ₅₀ (μM)		pK_a (4-hydroxy)	Anti-HIV activity μM ^a	
	pH 4.7	pH 6.2		CIC ₅₀	TC ₅₀
21	0.037	0.69	4.1	>69	69
27	0.26	0.30	6.0	28	67
29	0.15	0.36	6.2	25	67
32	0.23	0.20	ND ^b	14	70
42	0.014	0.097	4.0	69	76
47	0.0098	0.035	4.8	ND	

^aAntiviral assay using HIV-1_{IIIb} infected H9 cells.^bNot determined in this assay.

of in vitro inhibitory activity related to the deprotonation of the 4-hydroxyl of the compounds may contribute to the lack of antiviral activity, the data shown in Table 7 indicate that these inhibitors can be made much less pH sensitive and that antiviral activity can be achieved.

Conclusion

We were able to identify several small, achiral nonpeptidic HIV protease inhibitors with low micromolar activity that would be promising starting points for structure-based optimization. The most potent compound identified by the screen was the slow-binding inhibitor **5**, with $K_i=0.14$ μM. While an extensive effort has been employed elsewhere to optimize peptidic inhibitors, the mass screen hits we found indicate the value of such screening in identifying multiple nonpeptide HIV protease inhibitors in an efficient manner.

X-ray structural data indicated that the initial benzopyranones and pyranones bind at the active site, while displacing H₂O301. While optimization of the benzopyranones did not result in a dramatic improvement in inhibitory activity, the pyranones were modified by different strategies to yield highly potent inhibitors. Compound **19** achieves good activity (IC₅₀ = 160 nM, $K_i=51$ nM) by interacting in P1, P1' and potentially in P3. There are no literature reports of low nanomolar potency from a compound that reaches only three pockets in HIV protease, as is the case with **23** (IC₅₀ 7.0 = nM), which occupies P1, P1' and P2'. Pyranones that are branched at the 3-position offer an alternate strategy for reaching P1, P1' and P2'. While less potent than **23**, these compounds demonstrate micromolar anti-HIV activity. The dihydropyranones described provide examples of a strategy to successfully reach P1 and P2 from the 6-position of the pyranone template. The dihydropyranones **45**, **46**, and **47** occupy the four internal pockets P2–P2' and possess low nanomolar inhibitory activity. While these inhibitors are not more active than analogous pyranones at pH 4.7, the activity of the dihydropyranones is less pH sensitive.

The challenge that remains in optimizing these inhibitors is to achieve potent antiviral activity by improving in vitro activity and modifying physical properties that are potentially important to cellular activity (such as the 4-hydroxyl pK_a), while maintaining the nonpeptidic nature of the compounds. There are further indications of the value of these inhibitors as pharmacological agents. Thaisrivongs and co-workers²⁷ reported that a pyranone structurally similar to those reported here is highly bioavailable with a long half-life in rats and dogs. Also, we recently reported that the inhibitory activity of compound **21** is only weakly affected or unaffected by several HIV-1 protease point mutations reported to be associated with resistance to other HIV protease inhibitors.³¹ This finding suggests that antiviral pyranones or dihydropyranones may confer a pattern of resistance development that is different from that found for the peptidic protease inhibitors, which are to some extent cross-resistant.^{39,40} Thus, the compounds described have been optimized to yield high potency in vitro while remaining simple (one or no chiral centers) and nonpeptidic. Optimization now focuses on attaining high antiviral activity, with the knowledge that these compounds may have improved pharmacological characteristics over the peptidic HIV protease inhibitors currently in human clinical trials.

Experimental

HIV-1 Protease inhibition studies, anti-HIV assay

Inhibition of purified, recombinant HIV-1 protease was determined at pH 4.7 using the peptide substrate His-Lys-Ala-Arg-Val-Leu-(*p*-nitro-Phe)-Glu-Ala-Nle-Ser by an HPLC method as previously described.¹⁸ Protease concentrations used in the assays ranged from 0.45 to 1.5 nM. All inhibition assays were performed at pH 4.7, except where noted (Table 7). IC₅₀ determinations at pH 6.2 were performed in the same manner as pH 4.7 assays, except that the buffer used was 80 mM MES, 160 mM NaCl, 1.0 mM EDTA, 0.1% poly(ethylene glycol) (M_r 8000), pH 6.2. Selected pyranones and dihydropyranones were tested for antiviral activity (Table 7) using H9 cell infected with HIV-1_{IIIb}, as previously described.¹⁹

Chemistry

The procedure for preparation of the 4-hydroxy coumarins (compounds **1**, **8–15**) has been previously described.²⁰ Preparation of the 4-hydroxy-6-phenylpyranones has been previously described in two references (**2**, **16–19**,³⁰ **20–23**³¹). The preparation of 4-hydroxy-6-phenyl-pyranylthiomethanes (**24–32**) has also been previously described.¹⁹ Preparation of the dihydropyranones (**33–47**) has been described in detail in a Parke–Davis patent (WO.9514011-A2, and ref contained therein). The compounds were fully characterized by H NMR, CHN(S) analysis, MS and IR. Compounds **44** and **45** are pure enantiomers, prepared by asymmetric synthesis. The chirality of **44** and **45** was confirmed by an X-ray crystal structure of a synthetic

intermediate of each compound, and by the X-ray crystallographic structure of **45** bound to HIV-1 protease.

References

- Kohl, N. E.; Emini, E. A.; Schleif, W. A.; Davis, L. J.; Heimbach, J. C.; Dixon, R. A.; Scolnick, E. M.; Sigal, I. S. *Proc. Natl Acad. Sci. U.S.A.* **1990**, *85*, 4686.
- McQuade, T. J.; Tomasselli, A. G.; Liu, L.; Karacostas, V.; Moss, B.; Sawyer, T. K.; Heinrikson, R. L.; Tarpley, W. G. *Science* **1990**, *247*, 454.
- Davies, D. R. *Annu. Rev. Biophys. Biophys. Chem.* **1990**, *19*, 189.
- Greenlee, W. J. *Med. Res. Rev.* **1990**, *10*, 173.
- Wlodawer, A.; Erickson, J. W. *Annu. Rev. Biochem.* **1993**, *62*, 543.
- Appelt, K. In *Perspectives in Drug Discovery and Design. Therapeutic Approaches to HIV*; Anderson, P. S.; Kenyon, G. L.; Marshall, G. R., Eds.; ESCOM Science: Leiden, 1993; Vol. 1, pp 23–48.
- Huff, J. R. *J. Med. Chem.* **1991**, *34*, 2305.
- West, M. L.; Fairlie, D. P. *Trends Pharmacol. Sci.* **1995**, *16*, 67.
- Schechter, I.; Berger, A. *Biochem. Biophys. Res. Comm.* **1967**, *27*, 157.
- Plattner, J. J.; Norbeck, D. W. In *Drug Discovery Technologies*; Clark, C. R.; Moos, W. H., Eds.; Ellis Horwood: Chichester, 1990; pp 92–126.
- Roberts, N. A.; Martin, J. A.; Kinchington, D.; Broadhurst, A. V.; Craig, J. C.; Duncan, I. B.; Galpin, S. A.; Handa, B. K.; Kay, J.; Krohn, A.; Lambert, R. W.; Merrett, J. H.; Mills, J. S.; Parkes, K. E. B.; Redshaw, S.; Ritchie, A. J.; Taylor, D. L.; Thomas, G. J.; Machin, P. *Science* **1990**, *248*, 358.
- Vacca, J. P.; Dorsey, B. D.; Schleif, W. A.; Levin, R. B.; McDaniel, S. L.; Darke, P. L.; Zugay, J.; Quintero, J. C.; Blahy, O. M.; Roth, E.; Sardana, V. V.; Schlabach, A. J.; Graham, P. I.; Condra, J. H.; Gotlib, L.; Holloway, M. K.; Lin, J.; Chen, I. W.; Vastag, K.; Ostovic, D.; Anderson, P. S.; Emini, E. A.; Huff, J. R. *Proc. Natl Acad. Sci. U.S.A.* **1994**, *91*, 4096.
- Kempf, D. J.; Marsh, K. C.; Denissen, J. F.; McDonald, E.; Vasavanonda, S.; Flentge, C. A.; Green, B. E.; Fino, L.; Park, C. H.; Kong, X.; Wideburg, N. E.; Saldivar, A.; Ruiz, L.; Kati, W. M.; Sham, H. L.; Robins, T.; Stewart, K. D.; Hsu, A.; Plattner, J. J.; Leonard, J. M.; Norbeck, D. W. *Proc. Natl Acad. Sci. U.S.A.* **1995**, *92*, 2484.
- Lam, P. Y. S.; Jadhav, P. K.; Eyermann, C. J.; Hodge, C. N.; Ru, Y.; Bacheler, L. T.; Meek, J. L.; Otto, M. J.; Rayner, M. M.; Wong, Y. N.; Chang, C. H.; Weber, P. C.; Jackson, D. A.; Sharpe, T. R.; Ericksonviitanen, S. *Science* **1994**, *263*, 380.
- Tummino, P. J.; Ferguson, D.; Hupe, L.; Hupe, D. *Biochem. Biophys. Res. Comm.* **1994**, *200*, 1658.
- Thaisrivongs, S. In *Annual Reports in Medicinal Chemistry*; Bristol, J. A., Ed.; Academic: San Diego, 1994; Vol. 29, p 133.
- Bures, M. G.; Hutchins, C. W.; Maus, M.; Kohlbrenner, W.; Kadam, S.; Erickson, J. W. *Tetrahedron Comput. Methodol.* **1990**, *3*, 673.
- Tummino, P. J.; Ferguson, D.; Jacobs, C. M.; Tait, B.; Hupe, L.; Lunney, E.; Hupe, D. *Arch. Biochem. Biophys.* **1995**, *316*, 523.
- Vara Prasad, J. V. N.; Para, K. S.; Tummino, P. J.; Ferguson, D.; McQuade, T. J.; Lunney, E. A.; Rapundalo, S. T.; Batley, B. L.; Hingorani, G.; Domagala, J. M.; Gracheck, S. J.; Bhat, T. N.; Liu, B.; Baldwin, E. T.; Erickson, J. W.; Sawyer, T. K. *J. Med. Chem.* **1995**, *38*, 898.
- Lunney, E. A.; Hagen, S. E.; Domagala, J. M.; Humblet, C.; Kosinski, J.; Tait, B. D.; Warmus, J. S.; Wilson, M.; Ferguson, D.; Hupe, D.; Tummino, P. J.; Baldwin, E. T.; Bhat, T. N.; Liu, B. S.; Erickson, J. W. *J. Med. Chem.* **1994**, *37*, 2664.
- Suguna, K.; Padian, E. A.; Smith, C. W.; Carlson, W. D.; Davies, D. R. *Proc. Natl Acad. Sci. U.S.A.* **1987**, *84*, 7009.
- Swain, A. L.; Miller, M. M.; Green, J.; Rich, D. H.; Schneider, J.; Kent, S. B.; Wlodawer, A. *Proc. Natl Acad. Sci. U.S.A.* **1990**, *87*, 8805.
- Erickson, J.; Neidhart, D. J.; VanDrie, J.; Kempf, D. J.; Wang, X. C.; Norbeck, D. W.; Plattner, J. J.; Rittenhouse, J. W.; Turon, M.; Wideburg, N.; Kohlbrenner, W. E.; Simmer, R.; Helfrich, R.; Paul, D. A.; Knigge, M. *Science* **1990**, *249*, 527.
- Park, B. K. *Biochem. Pharmacol.* **1988**, *37*, 19.
- Tummino, P. J.; Ferguson, D.; Hupe, D. *Biochem. Biophys. Res. Comm.* **1994**, *201*, 290.
- Tomich, P.; Watenpaugh, K. Keystone Symposium Structural and Molecular Biology of Protease: Function and Inhibition, Sante Fe, New Mexico, 6–10 March 1994.
- Thaisrivongs, S.; Tomich, P. K.; Watenpaugh, K. D.; Chong, K. T.; Howe, W. J.; Yang, C. P.; Strohbach, J. W.; Turner, S. R.; McGrath, J. P.; Bohanon, M. J.; Lynn, J. C.; Mulichak, A. M.; Spinelli, P. A.; Hinshaw, R. R.; Pagano, P. J.; Moon, J. B.; Ruwart, M. J.; Wilkinson, K. F.; Rush, B. D.; Zipp, G. L.; Dalga, R. J.; Schwende, F. J.; Howard, G. M.; Padbury, G. E.; Toth, L. N.; Zhao, Z. Y.; Koeplinger, K. A.; Kakuk, T. J.; Cole, S. L.; Zaya, R. M.; Piper, R. C.; Jeffrey, P. *J. Med. Chem.* **1994**, *37*, 3200.
- Romines, K.; Watenpaugh, K. D.; Tomich, P. K.; Howe, W. J.; Morris, J. K.; Lovasz, K. D.; Mulichak, A. M.; Finzel, B. C.; Lynn, J. C.; Horng, M.; Schwende, F. J.; Ruwart, M. J.; Zipp, G. L.; Chong, K. T.; Dolak, L. A.; Toth, L. N.; Howard, G. M.; Rush, B. D.; Wilkinson, K. F.; Possert, P. L.; Dalga, R. J.; Hinshaw, R. R. *J. Med. Chem.* **1995**, *38*, 1884.
- Darke, P. L.; Nutt, R. F.; Brady, S. F.; Garsky, F. M.; Ciccarone, T. M.; Leu, C. T.; Lumma, P. K.; Freidinger, R. M.; Veber, D. F.; Sigal, I. S. *Biochem. Biophys. Res. Comm.* **1988**, *156*, 297.
- Vara Prasad, J. V. N.; Para, K. S.; Lunney, E. A.; Ortwine, D. F.; Dunbar, J. B.; Ferguson, D.; Tummino, P. J.; Hupe, D.; Tait, B. D.; Domagala, J. M.; Humblet, C.; Bhat, T. N.; Liu, B. S.; Guerin, D. M. A.; Baldwin, E. T.; Erickson, J. W.; Sawyer, T. K. *J. Am. Chem. Soc.* **1994**, *116*, 6989.
- Vara Prasad, J. V. N.; Lunney, E. A.; Ferguson, D.; Tummino, P. J.; Rubin, J. R.; Reynier, E. L.; Stewart, B. H.; Guttendorf, R. J.; Domagala, J. M.; Suvorov, L. I.; Gulnik, S. V.; Topol, I. A.; Bhat, T. N.; Erickson, J. W. *J. Am. Chem. Soc.* **1995**, *117*, 11070.

32. Konvalinka, J.; Strop, P.; Velek, J.; Cerna, V.; Kostka, V.; Philip, L. H.; Richards, A. D.; Dunn, B. M.; Kay, J. *FEBS Lett.* **1990**, *268*, 35.
33. Tait, B. The First Winter Conference on Medicinal and Bioorganic Chemistry, Steamboat Springs, CO, 29 Jan.–2 Feb. 1995.
34. Tait, B. 36th Buffalo Medicinal Chemistry Symposium, Buffalo, New York, 22 May 1995.
35. Hamilton, H.; Tait, B.; Ferguson, D.; Hagen, S.; Lunney, E.; Tummino, P. 210th ACS National Meeting, Chicago, Illinois, Aug. 1995.
36. Gajda, C.; Domagala, J.; Tait, B.; Hagen, S.; Tummino, P.; Ferguson, D.; Pavlovsky, A.; Rubin, J.; Lunney, E. 210th ACS National Meeting, Chicago, Illinois, Aug. 1995.
37. Hagen, S.; Domagala, J.; Ellsworth, E.; Ferguson, D.; Lunney, E.; Tait, B.; Tummino, P. 210th ACS National Meeting, Chicago, Illinois, Aug. 1995.
38. Hyland, L. J.; Tomaszek, T. J.; Meek, T. D. *Biochemistry* **1991**, *30*, 8454.
39. Condra, J. H.; Schleif, W. A.; Blahy, O. M.; Gabryelski, L. J.; Graham, D. J.; Quintero, J. C.; Rhodes, A.; Robbins, H. L.; Roth, E.; Shivaprakash, M.; Titus, D.; Yang, T.; Teppler, H.; Squires, K. E.; Deutsch, P. J.; Emini, E. A. *Nature* **1995**, *374*, 569.
40. Gulnik, S. V.; Suvorov, L. I.; Liu, B.; Yu, B.; Anderson, B.; Mitsuya, H.; Erickson, J. W. *Biochemistry* **1995**, *34*, 9282.
41. Longstaff, C.; Campbell, A. F.; Ferscht, A. R. *Biochemistry* **1990**, *29*, 7339.

(Received in U.S.A. 29 September 1995)